Received <day> <Month>, <year>; | Revised <day> <Month>, <year>; | Accepted <day> <Month>, <year>

DOI: xxx/xxxx

ARTICLE TYPE

Transition chaos in fractional order Cournot duopoly game model on scale-free network†

Fuat Gurcan*[1] | Senol Kartal[2] | Neriman Kartal[3]

[1]Department of Mathematics, Faculty of Science, Kuwait University, Safat,13060, Kuwait

[2]Department of Science and Mathematics Education, Nevsehir Haci Bektas Veli University, Nevsehir 50300, Turkey

[3]Department of Science and Mathematics Education, Nevsehir Haci Bektas Veli University, Nevsehir 50300, Turkey

Correspondence

*Fuat Gurcan, Department of Mathematics, Faculty of Science, Kuwait University, Safat,13060, Kuwait. Email: fuat.gurcan@ku.edu.kw

Present Address

Present address

Abstract

In this study, an Cournot duopoly model describing conformable fractional order differential equations with piecewise constant arguments is discussed. We have obtained two dimensional discrete dynamical system as a result of the discretization process is applied to the model. By using the center manifold theorem and the bifurcation theory, it is shown that the discrete dynamical system undergoes flip bifurcation about the Nash equilibrium point. Phase portraits, bifurcation diagrams, Lyaponov exponents show the existence of many complex dynamical behavior in the model such as stable equilibrium point, period-2 orbit, period-4 orbit, period-8 orbit, period-16 orbit and chaos according to changing the speed of adjustment parameter υ_1. Discrete Cournot duopoly game model is also considered on a Scale free network with $N = 10$ and $N = 100$ nodes. It is observed that the complex dynamical network exhibits similar dynamical behavior such as stable equilibrium point, Flip bifurcation and chaos depending on the changing the coupling strength parameter c_s. Moreover, flip bifurcation and transition chaos happen earlier in more heterogeneous networks. Calculating the Largest Lyapunov exponents guarantee the transition from nonchaotic to chaotic states in complex dynamical networks.

KEYWORDS:

Conformable fractional derivative ,Piecewise constant arguments, Stability, Flip bifurcation; Scale Free Network; Cournot duopoly game

1 | INTRODUCTION

Dynamical systems are mathematical tools that are frequently used in many fields such as population dynamics, physics, engineering and economics. In economy, researchers have proposed various mathematical models in order to explain competitive interaction between firms by using both discrete and continuous dynamical systems. An important part of these models have been focused on the interaction oligopolistic and duopoly markets. In 1838, Cournot proposed the first mathematical model describing the interaction between duopolistic markets. Complex dynamical behavior of Cournot model was studied by many researchers, such as, Agiza et al.[1], Aziza et al.[2] Yassen and Agiza[3], Agiza and Elsadany[4], Fanti and Gori[5], Fanti et al.[6], Zhu et al.[7], Gori et al.[8], Elsadany[9], Askar and Al kedhairi[10]. Agiza et al.[1] modeled a duopoly game with bounded rationality by using discrete dynamical systems. The stability and bifurcation analysis of the model reveal that Nash equilibrium point loses its stability via period-doubling bifurcation.

†This is an example for title footnote.

Researches have shown that memory and hereditary characteristics of the model that already exist in the natural structure of systems can be reflected by using the fractional-order derivative. These features cannot be reflected in integer order models and this situation leads to constitute a disadvantage in mathematical models. Considering this fact in the real world, many researchers have begun to prefer using fractional order derivative which are the generalization of classical derivatives to non-integer order [11,12,13,14,15].

Al-khedhairi studied the fractional order cournot duopoly game model with Caputo sense as follows:

$$\begin{cases} \frac{d^{\alpha}q_1(t)}{dt^{\alpha}} & = v_1 q_1(t)(a - c - 2q_1(t) - dq_2(t)) \\ \frac{d^{\alpha}q_2(t)}{dt^{\alpha}} & = v_2 q_2(t)(a - c - dq_1(t) - 2q_2(t)) \end{cases}. \tag{1}$$

Caputo and Riemann– Liouville fractional derivative is defined by means of an integral equation, and this also involves a big problem due to the non-local properties of this integral. This disadvantage leads to a weakness in modeling physical and biological phenomenon. In 2014, a new definition of fractional order derivative named conformable fractional derivative $(T_{\alpha}f)(t)$ has been presented in order to overcome these problems arising in Caputo fractional order derivative [16]. This derivative has some properties in connection with classical derivatives that are not in the Caputo fractional derivative [17]. For example, there is a relation between the left conformable fractional derivative starting from a and the classical derivative of the function f: $(T_{\alpha}^{a}f)(t) = (t-a)^{1-\alpha}f'(t)$.

Many physical and biological events in our world contain very large complex processes in their structures. In the mathematical modeling of this complex structures networks that consists of nodes and edges are used.Therefore, it is not surprising that researchers have shown so much interest to networks. In the literature, network that is the extension of graph theory has applications in many fields such as engineering [18], biology [19,20,21,22,23,24,25], economics [26], social science [27], physics [28], chemistry [29], computer science [30]. One of the most widely known and used types of networks is scale-free networks. Scale free network is a complex network where the number of connections per node(k)that is degree of a node has a power-law distribution. Complex network has non-trivial topological features that do not exist in simple networks. Analysis of the dynamical behavior of the complex network, such as synchronization, transition from non-chaotic to chaotic state as a result of bifurcation phenomena, is a hot topic and these dynamical behaviors gives us information about the complexity of the network. In the study [20,21], transition chaos with respect to coupling strength parameter has been reported for logistic map on both scale free and Erdos Renyi random network with $N = 1000$ nodes. Huang et al. [22] investigated dynamical behavior discrete time predator prey model on globally coupled network and observed rich dynamical behavior such as stable equilibrium point, Flip and Neimark-Sacker bifurcation and chaos in the complex network.

In this paper,we consider the following Cournot-type duopoly game model with conformable fractional order form where firms (players) produce homogeneous goods which are perfect substitutes and offer them at continuous-time periods $t = 0, 1, 2, ...$ on a common market.

$$\begin{cases} T^{a}q_1(t) & = v_1 q_1(t)(a - c - 2q_1(t) - dq_2(t)) \\ T^{a}q_2(t) & = v_2 q_2(t)(a - c - dq_1(t) - 2q_2(t)) \end{cases}. \tag{2}$$

where $q_i(t)$ is the output of firm i at time period t. The parameter a represent extend of market demand of both products, c is marginal cost of the players, v_i is speed parameters representing output adjustment.

2 | DISCRETIZATION PROCESS

In this section, we will discretize the model (2) based on approximation given in [31]. Firstly, we consider the model (2) with piecewise constant arguments as follows.

$$\begin{cases} T^{a}q_1(t) & = v_1 q_1([\frac{t}{h}]h)(a - c - 2q_1([\frac{t}{h}]h) - dq_2([\frac{t}{h}]h)) \\ T^{a}q_2(t) & = v_2 q_2([\frac{t}{h}]h)(a - c - dq_1([\frac{t}{h}]h) - 2q_2([\frac{t}{h}]h)) \end{cases}. \tag{3}$$

Applying the property of conformable fractional derivative $(T_{\alpha}^{a}f)(t) = (t-a)^{1-\alpha}f'(t)$ to the system (3) in the interval $t \in [nh, (n+1)h)$ leads to

$$\begin{cases} (t-nh)^{1-\alpha}\frac{dq_1(t)}{dt} & = v_1 q_1(nh)(a - c - 2q_1(nh) - dq_2(nh)) \\ (t-nh)^{1-\alpha}\frac{dq_2(t)}{dt} & = v_2 q_2(nh)(a - c - dq_1(nh) - 2q_2(nh)) \end{cases}. \tag{4}$$

By rearranging the system (4), one can holds

$$\begin{cases} dq_1(t) &= v_1 q_1(nh)(a-c-2q_1(nh)-dq_2(nh))(t-nh)^{\alpha-1}dt \\ dq_2(t) &= v_2 q_2(nh)(a-c-dq_1(nh)-2q_2(nh))(t-nh)^{\alpha-1}dt \end{cases}. \tag{5}$$

From the solutions of this system in the interval $t \in [nh, t)$, we obtain

$$\begin{cases} q_1(t)-q_1(nh) &= v_1 q_1(nh)(a-c-2q_1(nh)-dq_2(nh))\frac{(t-nh)^\alpha}{\alpha} \\ q_2(t)-q_2(nh) &= v_2 q_2(nh)(a-c-dq_1(nh)-2q_2(nh))\frac{(t-nh)^\alpha}{\alpha} \end{cases}. \tag{6}$$

Let $t \to (n+1)h$, then we have

$$\begin{cases} q_1((n+1)h)-q_1(nh) &= v_1 q_1(nh)(a-c-2q_1(nh)-dq_2(nh))\frac{h^\alpha}{\alpha} \\ q_2((n+1)h)-q_2(nh) &= v_2 q_2(nh)(a-c-dq_1(nh)-2q_2(nh))\frac{h^\alpha}{\alpha} \end{cases}. \tag{7}$$

Finally, to use an appropriate notation for the difference equations we replace $q_1(nh)$ and $q_2(nh)$ by $q_1(n)$ and $q_2(n)$. Therefore we obtain the following system of difference equations

$$\begin{cases} q_1(n+1) &= q_1(n)+v_1 q_1(n)(a-c-2q_1(n)-dq_2(n))\frac{h^\alpha}{\alpha} \\ q_2(n+1) &= q_2(n)+v_2 q_2(n)(a-c-dq_1(n)-2q_2(n))\frac{h^\alpha}{\alpha} \end{cases}. \tag{8}$$

3 | STABILITY ANALYSIS

Discrete dynamical system (8) has four equilibrium point $E_1 = (0,0)$, $E_2 = (\frac{a-c}{2}, 0)$, $E_3 = (0, \frac{a-c}{2})$ and $E^* = (q_1^*, q_2^*) = (\frac{a-c}{2+d}, \frac{a-c}{2+d})$. We note that E^* is the unique interior Nash equilibrium point that exists for $a > c$.

Theorem 1. If $a > c$ then the equilibrium point E_1 is source point.

Proof. The Jacobian matrix of the system (8) at $E_1 = (0,0)$ is

$$J(E_0) = \begin{pmatrix} 1+\frac{(a-c)h^\alpha v_1}{\alpha} & 0 \\ 0 & 1+\frac{(a-c)h^\alpha v_2}{\alpha} \end{pmatrix}$$

and has the eigenvalues: $\lambda_1 = 1+\frac{(a-c)h^\alpha v_1}{\alpha}$ and $\lambda_2 = 1+\frac{(a-c)h^\alpha v_2}{\alpha}$ It is easily seen that if $a > c$ then $|\lambda_{1,2}| > 1$ □

Theorem 2. If $a > c$ and $d \in (-1,1)$ then the equilibrium point E_2 is saddle point.

Proof. The Jacobian matrix of the system at $E_2 = (\frac{a-c}{2}, 0)$ is

$$J(E_1) = \begin{pmatrix} 1-\frac{(a-c)h^\alpha v_1}{\alpha} & -\frac{(a-c)dh^\alpha v_1}{2\alpha} \\ 0 & 1-\frac{(a-c)(-2+d)h^\alpha v_2}{2\alpha} \end{pmatrix}.$$

and has the eigenvalues: $\lambda_1 = 1-\frac{(a-c)h^\alpha v_1}{\alpha}$ and $\lambda_2 = 1+\frac{(a-c)h^\alpha v_2}{2\alpha}(2-d)$. The conditions $a > c$ and $d \in (-1,1)$ guarantee $|\lambda_1| < 1$ and $|\lambda_2| > 1$ respectively. □

Theorem 3. If $a > c$ and $d \in (-1,1)$ then the equilibrium point E_3 is saddle point.

Proof. The Jacobian matrix of the system at $E_3 = (0, \frac{a-c}{2})$ is

$$J(E_3) = \begin{pmatrix} 1-\frac{(a-c)(-2+d)h^\alpha v_1}{2\alpha} & 0 \\ -\frac{(a-c)dh^\alpha v_2}{2\alpha} & 1-\frac{(a-c)h^\alpha v_2}{\alpha} \end{pmatrix}.$$

and has the eigenvalues: $\lambda_1 = 1+\frac{(a-c)h^\alpha v_1}{2\alpha}(2-d)$ and $\lambda_2 = 1-\frac{(a-c)h^\alpha v_2}{\alpha}$. If $d \in (-1,1)$, then $|\lambda_1| > 1$ and if $a > c$, then $|\lambda_2| < 1$. □

Theorem 4. Suppose that $a > c$, $d \in (-1,1)$ and $0 < h^\alpha < \frac{(2+d)\alpha}{(a-c)v_2}$. If

$$v_1 < \frac{4\alpha((2+d)\alpha+(-a+c)h^\alpha v_2)}{(a-c)h^\alpha(4\alpha+(a-c)(-2+d)h^\alpha v_2)}. \tag{9}$$

then E^* is local asymptotically stable.

Proof. The Jacobian matrix of the system at $E^* = (q_1^*, q_2^*) = (\frac{a-c}{2+d}, \frac{a-c}{2+d})$ is

$$J(E^*) = \begin{pmatrix} 1 - \frac{2(a-c)h^\alpha v_1}{(2+d)\alpha} & \frac{(-a+c)dh^\alpha v_1}{(2+d)\alpha} \\ \frac{(-a+c)dh^\alpha v_2}{(2+d)\alpha} & 1 - \frac{2(a-c)h^\alpha v_2}{(2+d)\alpha} \end{pmatrix}.$$

Moreover, the characteristic polynomial of $J(E^*))$ is given by:

$$p(\lambda) = \lambda^2 + p_1\lambda + p_0 \tag{10}$$

where

$$p_1 = -2 + \frac{2(a-c)h^\alpha(v_1+v_2)}{(2+d)\alpha}. \tag{11}$$

and

$$p_0 = 1 - 2(v_1+v_2)\frac{h^\alpha(a-c)}{\alpha(d+2)} + v_1v_2(4-d)^2(\frac{h^\alpha(a-c)}{\alpha(d+2)})^2. \tag{12}$$

In order to obtain stability conditions for the characteristic polynomial (10) at the Nash equilibrium point E^* one can use the Schur-Cohn criterions that are:
a) $1 + p_1 + p_0 > 0$,
b) $1 - p_1 + p_0 > 0$
c) $1 - p_0 > 0$.
From the condition (a), we always hold

$$1 + p_1 + p_0 = v_1v_2(\frac{(a-c)h^\alpha}{(2+d)\alpha})^2(4-d)^2 > 0. \tag{13}$$

From (b) and (c) we have,

$$1 - p_1 + p_0 = 4 + \frac{(a-c)h^\alpha(-(a-c)(-2+d)h^\alpha v_1v_2 - 4\alpha(v_1+v_2))}{(2+d)\alpha^2} \tag{14}$$

and

$$1 - p_0 = \frac{(a-c)h^\alpha((a-c)(-2+d)h^\alpha v_1v_2 + 2\alpha(v_1+v_2))}{(2+d)\alpha^2}. \tag{15}$$

Considering the inequalities $a > c$, $d \in (-1, 1)$ and $0 < h^\alpha < \frac{(2+d)\alpha}{(a-c)v_2}$ with the fact (9), we have $1 - p_1 + p_0 > 0$ and $1 - p_0 > 0$. This completes our proof. □

4 | BIFURCATION ANALYSIS

In this section, we discuss the existence and direction of flip bifurcation for the system (8) at the Nash equilibrium point E^* by using the center manifold and bifurcation theory in [31,32,33,34,35,36]. The existence of Flip bifurcation needs the algebraic conditions that are
FB1) $1 + p_1 + p_0 > 0$
FB2) $1 - p_1 + p_0 = 0$
FB3) $p_1 \neq 0, 2$.
These three conditions guarantee $\lambda_1 = -1$ and $|\lambda_2| \neq 1$

Theorem 5. Suppose that the parameters satisfy $a \neq c$, $a \neq c + \frac{(2+d)\alpha}{h^\alpha v_2}$, $a \neq \frac{\pm\sqrt{d^2(-4+d^2)h^{2\alpha}\alpha^2v_2^2} + (-2+d)h^\alpha v_2((2+d)\alpha + ch^\alpha v_2)}{(-2+d)h^{2\alpha}v_2^2}$ and $n_{16} \neq 0$. If $v_1 = v_1^* = \frac{4\alpha((2+d)\alpha + (-a+c)h^\alpha v_2)}{(a-c)h^\alpha(4\alpha + (a-c)(-2+d)h^\alpha v_2)}$ then the system (8) undergoes Flip bifurcation at the equilibrium point (q_1^*, q_2^*). Morever, if $\alpha_2 > 0$ then the period-2 solution is stable, and if $\alpha_2 < 0$ then the period-2 solution is unstable.

Proof. From the FB1), we always holds $1 + p_1 + p_0 > 0$. From the solution of the equation in FB2, we obtain the critical Flip bifurcation point as

$$v_1 = v_1^* = \frac{4\alpha((2+d)\alpha + (-a+c)h^\alpha v_2)}{(a-c)h^\alpha(4\alpha + (a-c)(-2+d)h^\alpha v_2)}. \tag{16}$$

For the value of this v_1^*, the eigenvalues of the jacobian matrix are $\lambda_1 = -1$ and $\lambda_2 = \frac{4(2+d)\alpha^2 + (a-c)h^\alpha v_2(3(-4+d^2)\alpha - 2(a-c)(-2+d)h^\alpha v_2)}{(2+d)\alpha(4\alpha + (a-c)(-2+d)h^\alpha v_2)}$.
In addition if $a \neq c$, $a \neq c + \frac{(2+d)\alpha}{h^\alpha v_2}$ and $a \neq \frac{\pm\sqrt{d^2(-4+d^2)h^{2\alpha}\alpha^2v_2^2} + (-2+d)h^\alpha v_2((2+d)\alpha + ch^\alpha v_2)}{(-2+d)h^{2\alpha}v_2^2}$, then we have $p_1 \neq 0, 2$.

To decide the stability of the bifurcated period-2 points, we apply the center manifold reduction. Taking $\bar{v}_1$ as an independent variable into the system (8) and making transformation: $u = q_1 - q_1^*$, $v = q_2 - q_2^*$ ve $\bar{v}_1 = v_1 - v_1^*$, then the system (8) is transformed into:

$$\begin{pmatrix} u \\ \bar{v}_1 \\ v \end{pmatrix} \to \begin{pmatrix} \frac{(a-c)(4+d^2)h^\alpha v_2 - 4(2+d)\alpha}{(a-c)(-4+d^2)h^\alpha v_2 + 4(2+d)\alpha} & 0 & \frac{4(a-c)dv_2h^\alpha - 4d(2+d)\alpha}{(a-c)(-4+d^2)v_2h^\alpha + 4(2+d)\alpha} \\ 0 & 1 & 0 \\ -\frac{(a-c)dh^\alpha v_2}{(2+d)\alpha} & 0 & \frac{(h^\alpha v_2(2c-2a)+(2+d)\alpha)}{(2+d)\alpha} \end{pmatrix} \begin{pmatrix} u \\ \bar{v}_1 \\ v \end{pmatrix} + \begin{pmatrix} f_1(u,\bar{v}_1,v) \\ 0 \\ f_2(u,\bar{v}_1,v) \end{pmatrix} \tag{17}$$

where

$$\begin{aligned} f_1(u,\bar{v}_1,v) &= -\frac{2(a-c)h^\alpha}{(2+d)\alpha}ku - \frac{2h^\alpha}{\alpha}ku^2 - \frac{(a-c)dh^\alpha}{(2+d)\alpha}kv + \frac{8((a-c)h^\alpha v_2 - (2+d)\alpha)}{(a-c)((a-c)(-2+d)h^\alpha v_2 + 4\alpha)}u^2 \\ &\quad - \frac{4d(-(a-c)h^\alpha v_2 + (2+d)\alpha)}{(a-c)((a-c)(-2+d)h^\alpha v_2 + 4\alpha)}uv - \frac{dh^\alpha}{\alpha}ukv, \\ f_2(u,\bar{v}_1,v) &= -\frac{dh^\alpha v_2}{\alpha}uv - \frac{2h^\alpha v_2}{\alpha}v^2 \end{aligned}$$

Let

$$T = \begin{pmatrix} \frac{2(h^\alpha v_2(c-a)+(2+d)\alpha)}{(a-c)dh^\alpha v_2} & 0 & \frac{2d\alpha}{4\alpha + (a-c)(-2+d)h^\alpha v_2} \\ 0 & 1 & 0 \\ 1 & 0 & 1 \end{pmatrix}$$

and use the translation $\begin{pmatrix} u \\ \bar{v}_1 \\ v \end{pmatrix} = T \begin{pmatrix} X \\ \mu \\ Y \end{pmatrix}$. Then the map (17) becomes

$$\begin{pmatrix} X \\ \mu \\ Y \end{pmatrix} \to \begin{pmatrix} -1 & 0 & 0 \\ 0 & 1 & 0 \\ 0 & 0 & \frac{-2(a-c)^2(-2+d)h^{2\alpha}v_2^2 + 3(a-c)(-4+d^2)h^\alpha v_2\alpha + 4(2+d)\alpha^2}{\alpha((a-c)(-4+d^2)h^\alpha v_2 + 4(2+d)\alpha)} \end{pmatrix} \begin{pmatrix} X \\ \mu \\ Y \end{pmatrix} + \begin{pmatrix} F_1(X,\mu,Y) \\ 0 \\ F_2(X,\mu,Y) \end{pmatrix}, \tag{18}$$

where

$$\begin{aligned} F_1(X,\mu,Y) &= n_{11}XY + n_{12}Y^2 + n_{13}X^2 + n_{14}Y\mu + n_{15}Y^2\mu + n_{16}X\mu + n_{17}X^2\mu + n_{18}XY\mu \\ F_2(X,\mu,Y) &= n_{21}X^2 + n_{22}Y^2 + n_{23}XY + n_{24}X^2\mu + n_{25}XY\mu + n_{26}Y^2\mu + n_{27}X\mu + n_{28}Y\mu \end{aligned}$$

Let $z = (a-c)(-2+d)$. Then the Taylor coefficient can be computed as:

$$n_{11} = \frac{2d((a-c)^3(-4+d)^2v_2^3h^{3\alpha} - 2(a-c)^2(-4+d)^2v_2^2h^{2\alpha}\alpha + 4(a-c)(2+d)^2v_2h^{\alpha}\alpha^2 - 8(2+d)^2\alpha^3)}{(a-c)(zv_2h^{\alpha}+4\alpha)((a-c)zv_2^2h^{2\alpha} - 2(a-c)(-4+d^2)v_2h^{\alpha}\alpha - 4(2+d)\alpha^2)}$$

$$n_{12} = -\frac{2zd^2v_2^2h^{2\alpha}((-a+c)v_2h^{\alpha} + (2+d)\alpha)(zv_2h^{\alpha} + 2(2+d)\alpha)}{(zv_2h^{\alpha}+4\alpha)^2((a-c)zv_2^2h^{2\alpha} - 2(a-c)(-4+d^2)v_2h^{\alpha}\alpha - 4(2+d)\alpha^2)}$$

$$n_{13} = \frac{2(2+d)(zv_2h^{\alpha}+2(2+d)\alpha)(2(a-c)^2)v_2^2h^{2\alpha} + (a-c)(-4+d)(2+d)v_2h^{\alpha}\alpha + 4(2+d)\alpha^2)}{(a-c)^2dv_2h^{\alpha}((a-c)zv_2^2h^{2\alpha} - 2(a-c)(-4+d^2)v_2h^{\alpha}\alpha - 4(2+d)\alpha^2)}$$

$$n_{14} = -\frac{(a-c)^2zd^2v_2^2h^{3\alpha}}{-2(a-c)^2(-4+d^2)v_2^2h^{2\alpha}\alpha + 4(a-c)(-2+d)(2+d)^2v_2h^{\alpha}\alpha^2 + 8(2+d)^2\alpha^3}$$

$$n_{15} = -\frac{-(a-c)zd^3v_2^2h^{3\alpha}}{(a-c)z^2v_2^3h^{3\alpha} - 2(a-c)z(-6+d^2)v_2^2h^{2\alpha}\alpha - 12(a-c)(-4+d^2)v_2h^{\alpha}\alpha^2 - 16(2+d)\alpha^3}$$

$$n_{16} = -\frac{(a-c)h^{\alpha}(zv_2h^{\alpha}+4\alpha)^2}{-2(a-c)zv_2^2h^{2\alpha}\alpha + 4(a-c)(-4+d^2)v_2h^{\alpha}\alpha^2 + 8(2+d)\alpha^3}$$

$$n_{17} = \frac{(2+d)(zv_2h^{\alpha}+4\alpha)^2((-a+c)v_2h^{\alpha}+(2+d)\alpha)}{(a-c)dv_2\alpha((a-c)zv_2^2h^{2\alpha} - 2(a-c)(-4+d^2)v_2h^{\alpha}\alpha - 4(2+d)\alpha^2)}$$

$$n_{18} = \frac{((a-c)zdv_2^2h^{3\alpha} + 4d(2+d)h^{\alpha}\alpha^2)}{\alpha(-(a-c)zv_2^2h^{2\alpha} + 2(a-c)(-4+d^2)v_2h^{\alpha}\alpha + 4(2+d)\alpha^2)}$$

$$n_{21} = \frac{2(2+d)^2((a-c)v_2h^{\alpha}-2\alpha)(zv_2h^{\alpha}+4\alpha)((-a+c)v_2h^{\alpha}+(2+d)\alpha)}{(a-c)^2dv_2h^{\alpha}((a-c)zv_2^2h^{2\alpha} - 2(a-c)(-4+d^2)v_2h^{\alpha}\alpha - 4(2+d)\alpha^2)}$$

$$n_{22} = v_2h^{\alpha}(\frac{-2}{\alpha} + \frac{zd^3v_2h^{\alpha}}{(zv_2h^{\alpha}+4\alpha)^2} - \frac{2d(-2+d^2)}{zv_2h^{\alpha}+4\alpha}$$
$$+\frac{d((a-c)(-4+d^2)v_2h^{\alpha} - 2(-1+d)(2+d)^2\alpha)}{(a-c)zv_2^2h^{2\alpha} - 2(a-c)(-4+d^2)v_2h^{\alpha}\alpha - 4(2+d)\alpha^2})$$

$$n_{23} = (-\frac{(2+d)^2}{a-c} - \frac{2v_2h^{\alpha}}{\alpha} - \frac{d^3v_2h^{\alpha}}{zv_2h^{\alpha}+4\alpha}$$
$$+\frac{2dv_2h^{\alpha}(-(a-c)(-4+d^2)v_2h^{\alpha} + 2(-1+d)(2+d)^2\alpha)}{-(a-c)zv_2^2h^{2\alpha} + 2(a-c)(-4+d^2)v_2h^{\alpha}\alpha + 4(2+d)\alpha^2})$$

$$n_{24} = -\frac{(2+d)(zv_2h^{\alpha}+4\alpha)^2((-a+c)v_2h^{\alpha}+(2+d)\alpha)}{(a-c)dv_2\alpha((a-c)zv_2^2h^{2\alpha} - 2(a-c)(-4+d^2)v_2h^{\alpha}\alpha - 4(2+d)\alpha^2)}$$

$$n_{25} = -\frac{((a-c)zdv_2^2h^{3\alpha} + 4d(2+d)h^{\alpha}\alpha^2)}{\alpha(-(a-c)zv_2^2h^{2\alpha} + 2(a-c)(-4+d^2)v_2h^{\alpha}\alpha + 4(2+d)\alpha^2)}$$

$$n_{26} = \frac{(a-c)zd^3v_2^2h^{3\alpha}}{(a-c)z^2v_2^3h^{3\alpha} - 2(a-c)z(-6+d^2)v_2^2h^{2\alpha}\alpha - 12(a-c)(-4+d^2)v_2h^{\alpha}\alpha^2 - 16(2+d)\alpha^3}$$

$$n_{27} = \frac{(a-c)h^{\alpha}(zv_2h^{\alpha}+4\alpha)^2}{-2(a-c)zv_2^2h^{2\alpha}\alpha + 4(a-c)(-4+d^2)v_2h^{\alpha}\alpha^2 + 8(2+d)\alpha^3}$$

$$n_{28} = \frac{(a-c)^2zd^2v_2^2h^{3\alpha}}{-2(a-c)^2(-4+d^2)v_2^2h^{2\alpha}\alpha + 4z(2+d)^2v_2h^{\alpha}\alpha^2 + 8(2+d)^2\alpha^3}$$

Suppose that

$$W^c(0) = \{(X,\mu,Y) \in R^3 | Y = h^*(X,\mu), h^*(0,0) = 0, Dh^*(0,0) = 0\}$$

is the center manifold for the system of $(X,Y) = (0,0)$ near $\mu = 0$.

Assume that

$$h^*(X,\mu) = AX^2 + BX\mu + G\mu^2 + O((|X| + |\mu|)^3).$$

By approximate computation for the center manifold, we have

$$\begin{aligned} A &= \frac{(2+d)\alpha(zv_2h^\alpha + 4\alpha)n_{21}}{2zv_2h^\alpha((a-c)v_2h^\alpha - (2+d)\alpha)} \\ B &= \frac{(2+d)\alpha(zv_2h^\alpha + 4\alpha)n_{27}}{2(a-c)zv_2^2h^{2\alpha} - 4(a-c)(-4+d^2)v_2h^\alpha\alpha - 8(2+d)\alpha^2} \\ G &= 0 \end{aligned}$$

Now, the map (17) restricted to the center manifold is given by

$$\tilde{F} : X \to -X + h_1X^2 + h_2X\mu + h_3\mu^2 + h_4X^3 + h_5X^2\mu + h_6X\mu^2 + h_7\mu^3 + O((|X| + |\mu|)^4) \tag{19}$$

where

$$\begin{aligned} h_1 &= n_{13} \\ h_2 &= n_{16} \\ h_3 &= h_7 = 0 \\ h_4 &= \frac{(2+d)\alpha(zv_2h^\alpha + 4\alpha)n_{11}n_{21}}{2zv_2h^\alpha((a-c)v_2h^\alpha - (2+d)\alpha)} \\ h_5 &= \frac{1}{2}(2n_{17} + (2+d)\alpha(zv_2h^\alpha + 4\alpha)(\frac{n_{14}n_{21}}{zv_2h^\alpha((a-c)v_2h^\alpha - (2+d)\alpha)} \\ &\quad + \frac{n_{11}n_{27}}{(a-c)zv_2^2h^{2\alpha} - 2(a-c)(-4+d)^2v_2h^\alpha\alpha - 4(2+d)\alpha^2})) \\ h_6 &= \frac{(2+d)\alpha(zv_2h^\alpha + 4\alpha)n_{14}n_{27}}{2(a-c)zv_2^2h^{2\alpha} - 4(a-c)(-4+d^2)v_2h^\alpha\alpha - 8(2+d)\alpha^2} \end{aligned}$$

As given by the flip bifurcation theorem in[36], the emergence of flip bifurcation for map (18) requires

$$\begin{aligned} \alpha_1 &= \left[\frac{\partial F}{\partial\mu}.\frac{\partial^2 F}{\partial X^2} + 2\frac{\partial^2 F}{\partial X\partial\mu}\right]\Big|_{(0,0)} = 2n_{16} \neq 0 \\ \alpha_2 &= \left[\frac{1}{2}.\left(\frac{\partial^2 F}{\partial X^2}\right)^2 + \frac{1}{3}.\frac{\partial^3 F}{\partial X^3}\right]\Big|_{(0,0)} = \frac{2+d}{(a-c)^4v_2^2h^{2\alpha}}x(\\ &\quad \frac{8(2+d)(zv_2h^\alpha + 2(2+d)\alpha)^2(2(a-c)^2v_2^2h^{2\alpha} + (a-c)(-4+d)(2+d)v_2h^\alpha\alpha + 4(2+d)\alpha^2)^2}{d^2((a-c)zv_2^2h^{2\alpha} - 2(a-c)(-4+d^2)v_2h^\alpha\alpha - 4(2+d)\alpha^2)^2} \\ &\quad + \frac{(a-c)^3v_2h^\alpha\alpha(zv_2h^\alpha + 4\alpha)n_{11}n_{21}}{(-2+d)((a-c)v_2h^\alpha - (2+d)\alpha)}) \neq 0 \end{aligned}$$

Thus, the proof is completed. □

5 | COURNOT DUOPOLY GAME MODEL ON SCALE FREE NETWORK

In this section, we consider Cournot duopoly game model on Scale Free Network. Let a node of a network given by following two-dimensional discrete dynamical system.

$$\begin{cases} x(k+1) = x(k) + v_1x(k)(a - c - 2x(k) - dy(k))\frac{h^\alpha}{\alpha} = f(x(k), y(k)) \\ y(k+1) = y(k) + v_2y(k)(a - c - dx(k) - 2y(k))\frac{h^\alpha}{\alpha} = g(x(k), y(k)) \end{cases}. \tag{20}$$

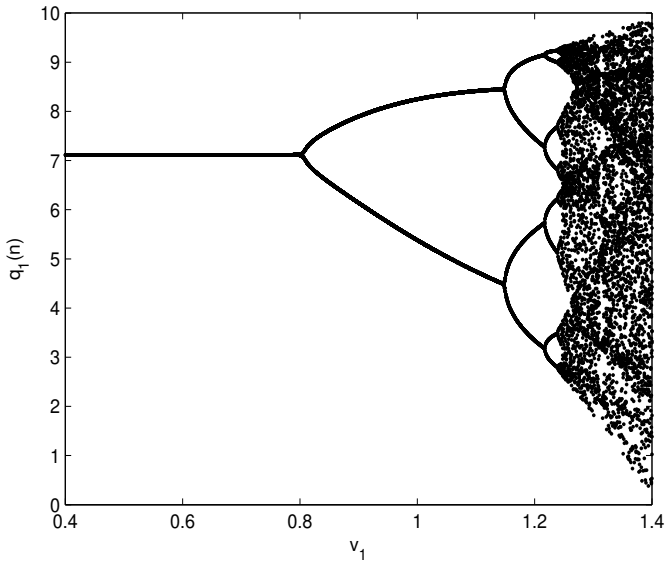

FIGURE 1 Flip bifurcation diagram of the system (8) at the Nash equilibrium point for the parameter values $a = 19$, $c = 0,5$,$d = 0.6$, $\upsilon_2 = 1$, $h = 0.1$ and $\alpha = 0.95$.

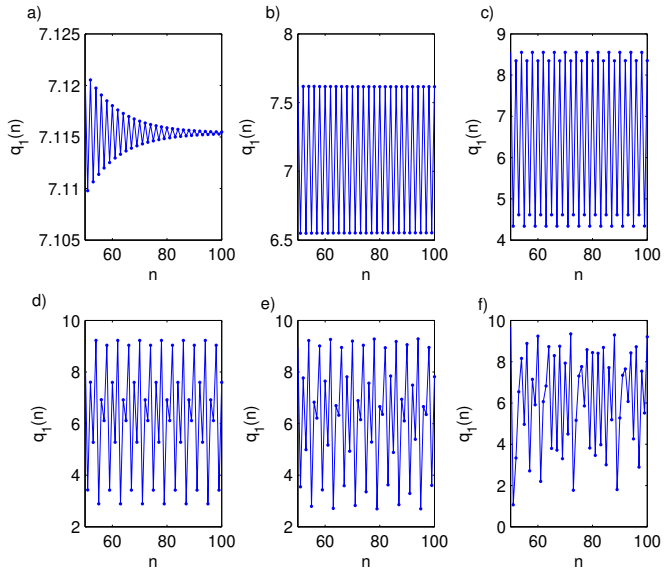

FIGURE 2 Time series plot of model (8) with respect to parameter υ_1: (a) stable equilibrium point for $\upsilon_1 = 0.7$, (b) period-2 orbit for $\upsilon_1 = 0.85$, (c) period-4 orbit for $\upsilon_1 = 1.15$, (d) period-8 orbit for $\upsilon_1 = 1.23$, (d) period-16 orbit for $\upsilon_1 = 1.244$, (f) chaos for $\upsilon_1 = 1.35$.

If we take into account N connected coupled identical nodes in network, then state equations of this network are given as follows:

$$\begin{cases} x_i(k+1) = f(x_i(k), y_i(k)) - c_s \sum_{j=1}^{N} a_{ij} f(x_j(k), y_j(k)) \\ y_i(k+1) = g(x_i(k), y_i(k)) - c_s \sum_{j=1}^{N} a_{ij} g(x_j(k), y_j(k)) \end{cases} \tag{21}$$

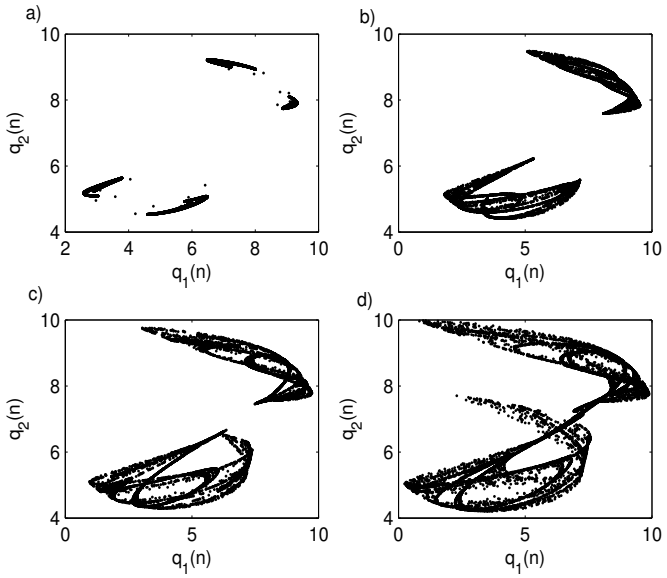

FIGURE 3 Phase portrait of the system (8) with respect to parameter v_1: (*a*) $v_1 = 1.25$, (*b*) $v_1 = 1.3$, (*c*) $v_1 = 1.35$, (*d*) $v_1 = 1.39$.

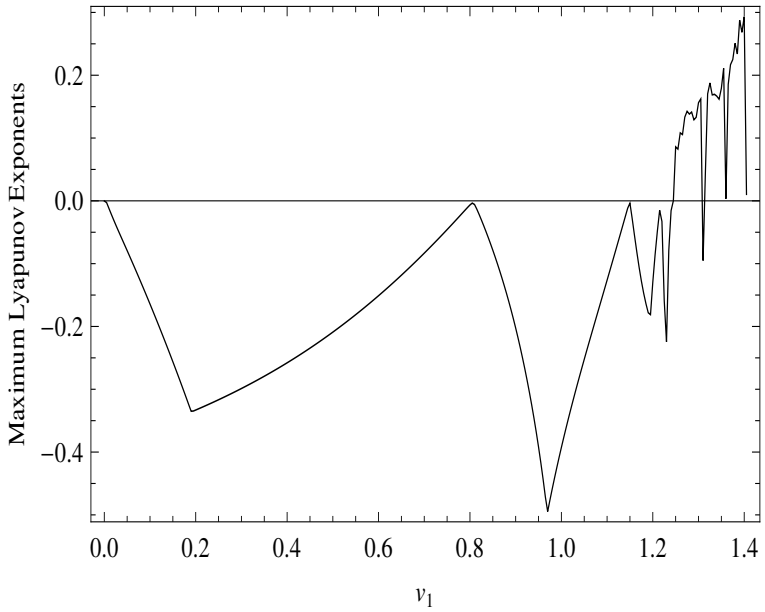

FIGURE 4 Maximum Lyapunov exponents with changing the parameter v_1.

where i and j are the sequence number of the nodes in the coupled dynamical network, c_s is the coupling strength of the network. The coupling matrix $A \in R^{NxN}$ can be expressed by

$$A = \begin{pmatrix} d_{11} & a_{12} & a_{13} & \dots & a_{1N} \\ a_{12} & d_{22} & a_{23} & \dots & a_{2N} \\ a_{13} & a_{23} & d_{33} & \dots & a_{3N} \\ \vdots & \vdots & \vdots & \ddots & \dots \\ a_{1N} & a_{2N} & a_{3N} & \dots & d_{NN} \end{pmatrix} \tag{22}$$

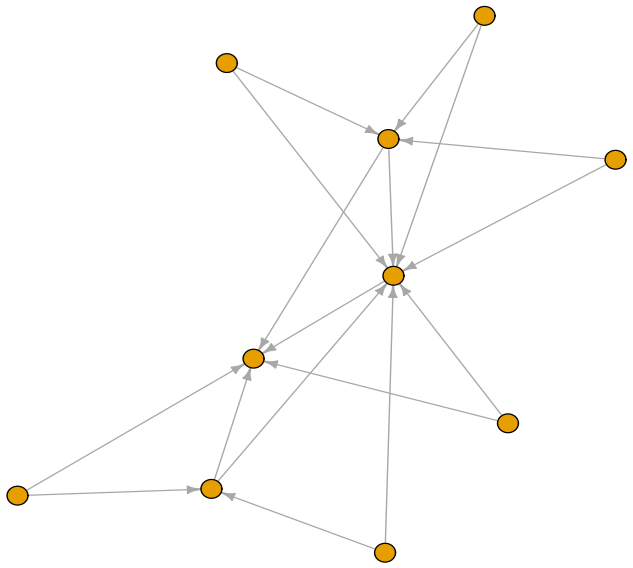

FIGURE 5 Scale free network with $N = 10$ nodes.

If there is a connection between node i and j, then $a_{ij} = 1$; otherwise, $a_{ij} = 0 (i \neq j)$. Let $a_{ii} = -d_i$, $i = 1, 2, ..., N$, where d_i is the degree of node i and can be defined by the following equation:

$$d_{ii} = -\sum_{j=1, j\neq i}^{N} a_{ij} = -\sum_{j=1, j\neq i}^{N} a_{ji}$$

A matrix form of system (21) is

$$\begin{cases} X_{k+1} = (I - cA) f(X(k), Y(k)) \\ Y_{k+1} = (I - cA) g(X(k), Y(k)) \end{cases} . \tag{23}$$

where $X_k = (x_1(k), x_2(k), ..., x_N(k))$, $Y_k = (y_1(k), y_2(k), ..., y_N(k))$ and $I \in R^{Nxn}$ is identity matrix.

6 | NUMERICAL SIMULATIONS

In this section, we give some numerical simulations of the theoretical results obtained in section 3, section 4 and section 5. Theorem 1, Theorem 2 and Theorem 3 present algebraic conditions for local asymptotically stable of the equilibrium points $E_1 = (0, 0)$, $E_2 = (\frac{a-c}{2}, 0)$, $E_3 = (0, \frac{a-c}{2})$ respectively. Since these equilibrium points have no economic implications, their mathematical consequences will not be discussed. Now we focus on the Nash equilibrium point $E^* = (q_1^*, q_2^*) = (\frac{a-c}{2+d}, \frac{a-c}{2+d})$ that is very important to market economy. Theoretical results show that speed of adjustment parameter υ_1 plays a key role on the dynamics of market. Theorem 4 gives the stability region for the Nash equilibrium point E^* with respect to parameter υ_1. For the numerical simulations we choose the parameter as $a = 19$, $c = 0.5$, $d = 0.6$, $\upsilon_2 = 1$, $h = 0.1$ and $\alpha = 0.95$. Inequality (9) gives stable region with respect to parameter υ_1 as $\upsilon_1 < 0.807378$. In section 5, we deal with the Flip bifurcation analysis by using center manifold theory about the Nash equilibrium point E^*. For this purpose the parameter υ_1 select as a Flip bifurcation parameter due to above fact. The critical value of speed of adjustment parameter υ_1^* for this bifurcation is given (16). For the above parameter values we get this value as $\upsilon_1^* = 0.807378$. In addition for this critical value the jacobian matrix has the eigenvalues $\lambda_1 = -1$ and $\lambda_2 = -0.0377623$. On the other hand we holds $a \neq 0.5$, $a \neq 23.6725$ and $\alpha_1 = -0.00714402 \neq 0$ and $\alpha_2 = 0.0879606 \neq 0$. Now all of the conditions of Flip bifurcation satisfy and this bifurcation emerge about the Nash equilibrium point $E^* = (7.11538, 7.11538)$ (Figure 1). Moreover, discrete dynamical system exhibit more complex phenomena by increasing the value of υ_1 about the Nash equilibrium point such as stable equilibrium point for $\upsilon_1 = 0.7$, period-2 orbit for $\upsilon_1 = 0.85$, period-4 orbit for $\upsilon_1 = 1.15$, period-8 orbit for $\upsilon_1 = 1.23$, period-16 orbit for $\upsilon_1 = 1.244$ and chaos for $\upsilon_1 = 1.35$. We note that period-2 solutions is stable because we hold $\alpha_2 > 0$ (Figure 2). Figure 3 shows the chaotic attractor with respect

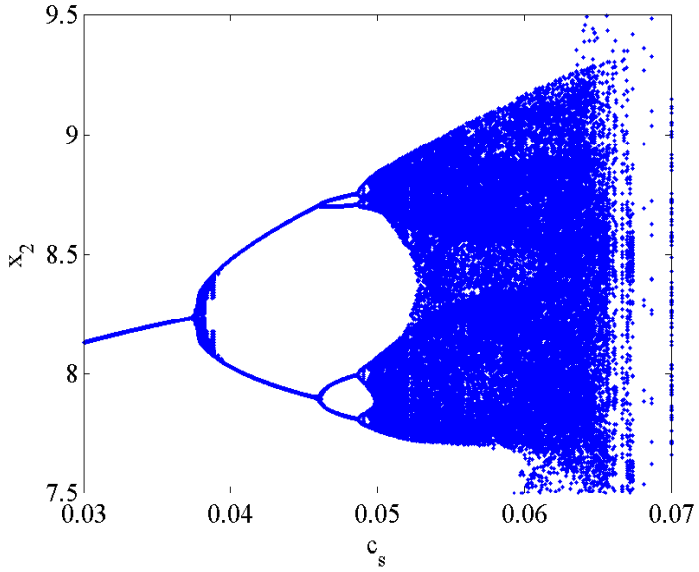

FIGURE 6 Complex dynamics of the discrete Cournot duopoly game model on scale free network with $N = 10$ nodes.

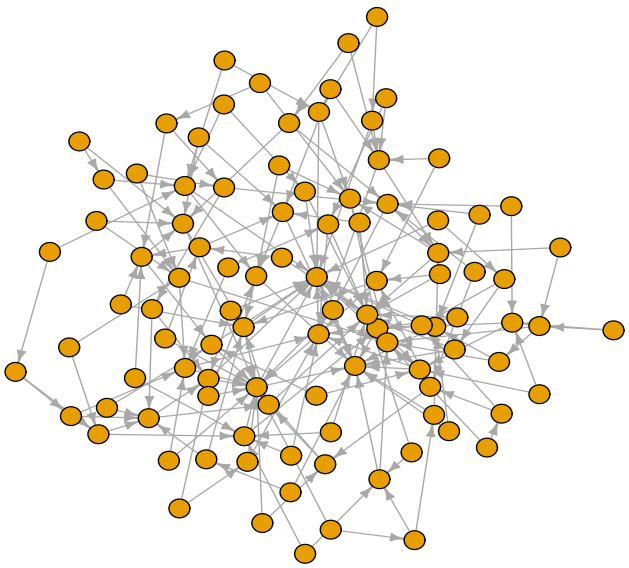

FIGURE 7 Scale free network with $N = 100$ nodes.

to increasing the speed of adjustment parameter where $v_1 = 1.25$, $v_1 = 1.3$, $v_1 = 1.35$ and $v_1 = 1.39$. Figure 4 shows the maximum Lyapunov exponent according the changing the parameter v_1 where some Lyapunov exponents are bigger than 0, some are smaller than 0. Positive Lyapunov exponent guarantees the existence of chaotic motion for discrete dynamical system about Nash equilibrium point.

In section 5, we also study the discrete time cournot duopoly game model (8) on scale free network with the parameter $a = 19$, $c = 0.5$, $d = 0.6$, $v_2 = 1$, $h = 0.1$, $\alpha = 0.95$ and $v_1 = 0.75$ that are not located in chaotic regions. If the dynamics of each node can represent cournot-duopoly game model (20), then dynamics of N connected coupled identical nodes in scale free network are given N-dimensional system of difference equations (21). Such a network can be viewed as a product output market

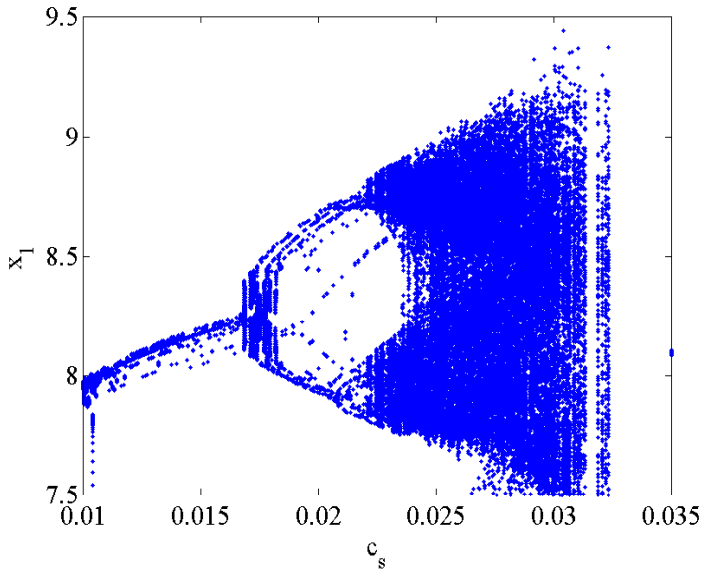

FIGURE 8 Complex dynamics of Cournot duopoly game model on scale free network with $N = 100$ nodes.

competition based on the interaction between two chain markets. For the numerical simulations, we use scale free network with $N = 10$ and $N = 100$ nodes respectively which are plotted in Figure 5 and Figure 7.

In order to see the complex dynamical behavior of network with $N = 10$ nodes we focus on the nodes in networks with the highest degree, which for is 2 and its degree is 8. So we plot the bifurcation diagram with respect to parameter coupling strength of the network c_s against to x_2 where the coupling matrix C is

$$A = \begin{pmatrix} -5 & 1 & 1 & 0 & 1 & 1 & 1 & 0 & 0 & 0 \\ 1 & -8 & 1 & 1 & 1 & 0 & 1 & 1 & 1 & 1 \\ 1 & 1 & -4 & 1 & 0 & 1 & 0 & 0 & 0 & 0 \\ 0 & 1 & 1 & -2 & 0 & 0 & 0 & 0 & 0 & 0 \\ 1 & 1 & 0 & 0 & -5 & 0 & 0 & 1 & 1 & 1 \\ 1 & 0 & 1 & 0 & 0 & -2 & 0 & 0 & 0 & 0 \\ 1 & 1 & 0 & 0 & 0 & 0 & -2 & 0 & 0 & 0 \\ 0 & 1 & 0 & 0 & 1 & 0 & 0 & -2 & 0 & 0 \\ 0 & 1 & 0 & 0 & 1 & 0 & 0 & 0 & -2 & 0 \\ 0 & 1 & 0 & 0 & 1 & 0 & 0 & 0 & 0 & -2 \end{pmatrix}$$

Figure 6 shows that if the coupling parameter c_s reaches the some critical value where it is interval $c_s \in [0.03, 0.04]$, then Flip bifurcation occurs about the positive equilibrium point. In addition, complex dynamical network exhibit similar dynamical behavior with respect to parameter c_s such as stable equilibrium point for $c_s = 0.06$, period-2 orbit for $c_s = 0.037$, period-4 orbit for $c_s = 10.045$, period-8 orbit for $c_s = 0.048$, period-16 orbit for $c_s = 0.049$ and chaos for $c_s = 0.055$ (Figure 9). Then, we again examine the dynamics of the network with $N = 100$ nodes by increasing the number of nodes with the highest degree, which for is 1 and its degree is 17. Figure 8 shows that Flip bifurcation occurs at a smaller value of c_s in the complex dynamical network with $N = 100$ nodes where it is in range $c_s \in [0.015, 0.02]$. So, we can say that as the number of node increases, bifurcation occur at a lower coupling strength parameter c_s.

In addition we also calculate Largest Lyapunov Exponent in order to see the chaotic motion in scale free network with $N = 10$ nodes and $N = 100$ nodes. The procedure calculating the Largest Lyapunov Exponent is first introduced in study [37,38] and based on procedure that use the least squares method to fit line to the slope of the natural logarithm of the absolute value of lower bound error. In Figure 10 the slop of the red line is the Largest Lyapunov Exponents that are 0.337 and 0.309 for $N = 10$ nodes and $N = 100$ nodes respectively. Largest Lyapunov exponents provide evidence for the existence of chaos in complex dynamical network.

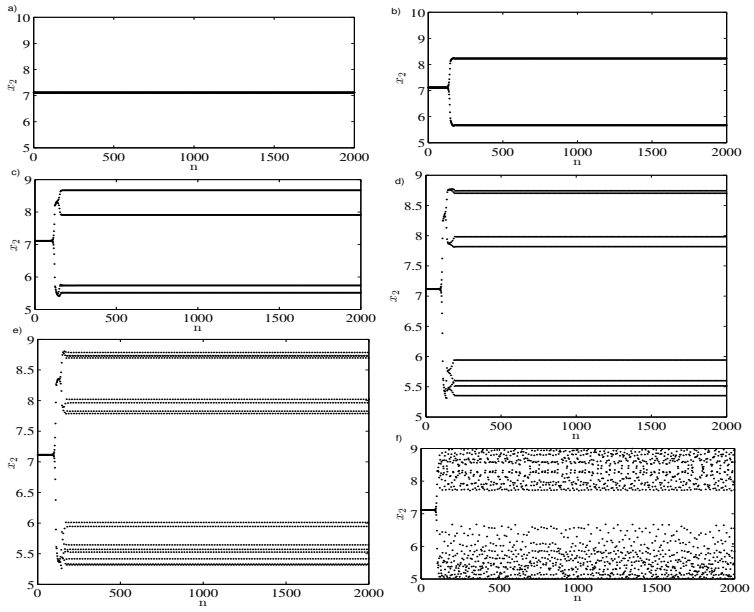

FIGURE 9 Dynamical behavior of scale free network with $N = 10$ node on Cournot duopoly game model. (a) stable equilibrium point for $c_s = 0.06$, (b) period-2 orbit for $c_s = 0.037$, (c) period-4 orbit for $c_s = 0.045$, (d) period-8 orbit for $c_s = 0.048$, (e) period-16 orbit for $c_s = 0.049$, (f) chaos for $c_s = 0.055$.

7 | CONCLUSIONS

In this work, we have studied cournot-duopoly game model via conformable fractional order form with piecewise constant arguments. From the solutions of the model with piecewise constant arguments gives us two dimensional system of difference equations. Phase portrait, bifurcation diagrams and positive Lyapunov exponents indicate that discrete model displays many complex dynamical behavior about the Nash equilibrium point such as stable equilibrium point, period-2 orbit, period-4 orbit, period-8 orbit, period-16 orbit and chaos according to changing the speed of adjustment parameter v_1. Discrete cournot-duopoly game model is also considered on the scale free network with $N = 10$ and $N = 100$ nodes. In this situation we investigate the effect of the coupling strength parameter c_s on the dynamical behavior of the complex network where the other parameters are not located in chaotic region. Bifurcation diagrams show that there exists the transition from non-chaotic states to chaotic state in the networks depending on the parameter c_s. Calculating the largest Lyapunov exponents confirm the existence of chaos for the complex networks.

7.1 | Bibliography

References

1. Agiza H, Hegazi A, Elsadany A. Complex dynamics and synchronization of a duopoly game with bounded rationality. *Mathematics and Computers in Simulation* 2002; 58(2): 133–146. doi: 10.1016/s0378-4754(01)00347-0

2. Agiza H, Hegazi A, Elsadany A. The dynamics of Bowley's model with bounded rationality. *Chaos, Solitons &amp Fractals* 2001; 12(9): 1705–1717. doi: 10.1016/s0960-0779(00)00021-7

3. Yassen M, Agiza H. Analysis of a duopoly game with delayed bounded rationality. *Applied Mathematics and Computation* 2003; 138(2-3): 387–402. doi: 10.1016/s0096-3003(02)00143-1

4. Agiza H, Elsadany A. Nonlinear dynamics in the Cournot duopoly game with heterogeneous players. *Physica A: Statistical Mechanics and its Applications* 2003; 320: 512–524. doi: 10.1016/s0378-4371(02)01648-5

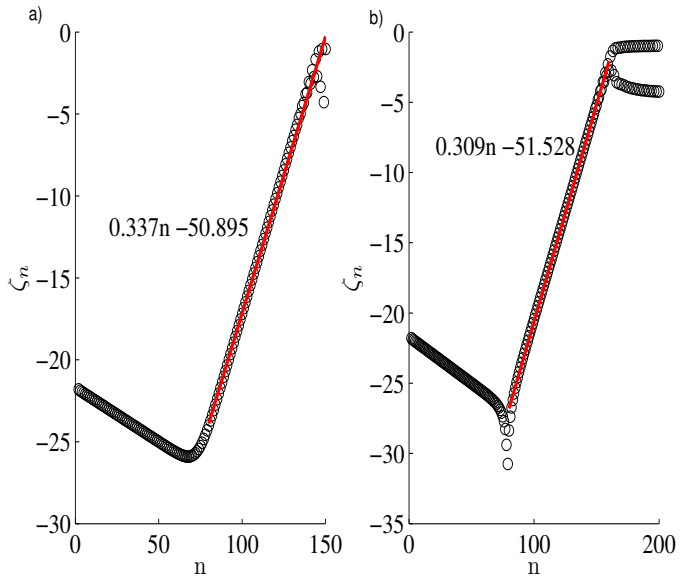

FIGURE 10 Computation of the largest positive Lyapunov exponent to the node with the highest degree in scale free network. (a) $N = 10$ nodes (b) $N = 100$ nodes.

5. Fanti L, Gori L. The dynamics of a differentiated duopoly with quantity competition. *Economic Modelling* 2012; 29(2): 421–427. doi: 10.1016/j.econmod.2011.11.010

6. Fanti L, Gori L, Sodini M. Nonlinear dynamics in a Cournot duopoly with relative profit delegation. *Chaos, Solitons &amp Fractals* 2012; 45(12): 1469–1478. doi: 10.1016/j.chaos.2012.08.008

7. Zhu X, Zhu W, Yu L. Analysis of a nonlinear mixed Cournot game with boundedly rational players. *Chaos, Solitons &amp Fractals* 2014; 59: 82–88. doi: 10.1016/j.chaos.2013.11.013

8. Gori L, Guerrini L, Sodini M. A continuous time Cournot duopoly with delays. *Chaos, Solitons &amp Fractals* 2015; 79: 166–177. doi: 10.1016/j.chaos.2015.01.020

9. Elsadany A. Dynamics of a Cournot duopoly game with bounded rationality based on relative profit maximization. *Applied Mathematics and Computation* 2017; 294: 253–263. doi: 10.1016/j.amc.2016.09.018

10. Askar S, Al-khedhairi A. Dynamic investigations in a duopoly game with price competition based on relative profit and profit maximization. *Journal of Computational and Applied Mathematics* 2020; 367: 112464. doi: 10.1016/j.cam.2019.112464

11. Al-khedhairi A. Differentiated Cournot duopoly game with fractional-order and its discretization. *Engineering Computations* 2019; 36(3): 781–806. doi: 10.1108/ec-07-2018-0333

12. Li P, Yan J, Xu C, Gao R, Li Y. Understanding Dynamics and Bifurcation Control Mechanism for a Fractional-Order Delayed Duopoly Game Model in Insurance Market. *Fractal and Fractional* 2022; 6(5): 270. doi: 10.3390/fractalfract6050270

13. Xin B, Peng W, Guerrini L. A Continuous Time Bertrand Duopoly Game With Fractional Delay and Conformable Derivative: Modeling, Discretization Process, Hopf Bifurcation, and Chaos. *Frontiers in Physics* 2019; 7. doi: 10.3389/fphy.2019.00084

14. Al-Khedhairi A, Elsadany AA, Elsonbaty A. On the Dynamics of a Discrete Fractional-Order Cournot–Bertrand Competition Duopoly Game. *Mathematical Problems in Engineering* 2022; 2022: 1–13. doi: 10.1155/2022/8249215

15. Khennaoui AA, Almatroud AO, Ouannas A, Al-sawalha MM, Grassi G, Pham VT. The effect of caputo fractional difference operator on a novel game theory model. *Discrete &amp Continuous Dynamical Systems - B* 2021; 26(8): 4549. doi: 10.3934/dcdsb.2020302

16. Khalil R, Horani MA, Yousef A, Sababheh M. A new definition of fractional derivative. *Journal of Computational and Applied Mathematics* 2014; 264: 65–70. doi: 10.1016/j.cam.2014.01.002

17. Abdeljawad T. On conformable fractional calculus. *Journal of Computational and Applied Mathematics* 2015; 279: 57–66. doi: 10.1016/j.cam.2014.10.016

18. Saleh M, Esa Y, Mohamed A. Applications of Complex Network Analysis in Electric Power Systems. *Energies* 2018; 11(6): 1381. doi: 10.3390/en11061381

19. Koutrouli M, Karatzas E, Paez-Espino D, Pavlopoulos GA. A Guide to Conquer the Biological Network Era Using Graph Theory. *Frontiers in Bioengineering and Biotechnology* 2020; 8. doi: 10.3389/fbioe.2020.00034

20. Nepomuceno EG, Perc M. Computational chaos in complex networks. *Journal of Complex Networks* 2019. doi: 10.1093/comnet/cnz015

21. Li X, Chen G, Ko KT. Transition to chaos in complex dynamical networks. *Physica A: Statistical Mechanics and its Applications* 2004; 338(3-4): 367–378. doi: 10.1016/j.physa.2004.02.010

22. Huang T, Zhang H, Ma S, Pan G, Wang Z, Huang H. Bifurcations, Complex Behaviors, and Dynamic Transition in a Coupled Network of Discrete Predator-Prey System. *Discrete Dynamics in Nature and Society* 2019; 2019: 1–22. doi: 10.1155/2019/2583730

23. Ahmed E, Matouk AE. Complex dynamics of some models of antimicrobial resistance on complex networks. *Mathematical Methods in the Applied Sciences* 2020; 44(2): 1896–1912. doi: 10.1002/mma.6889

24. Zhang HF, Wu RX, Fu XC. The emergence of chaos in complex dynamical networks. *Chaos, Solitons &amp Fractals* 2006; 28(2): 472–479. doi: 10.1016/j.chaos.2005.07.001

25. Wang Z, Jiang G, Yu W, He W, Cao J, Xiao M. Synchronization of coupled heterogeneous complex networks. *Journal of the Franklin Institute* 2017; 354(10): 4102–4125. doi: 10.1016/j.jfranklin.2017.03.006

26. Emmert-Streib F, Tripathi S, Yli-Harja O, Dehmer M. Understanding the World Economy in Terms of Networks: A Survey of Data-Based Network Science Approaches on Economic Networks. *Frontiers in Applied Mathematics and Statistics* 2018; 4. doi: 10.3389/fams.2018.00037

27. Kasper C, Voelkl B. A social network analysis of primate groups. *Primates* 2009; 50(4): 343–356. doi: 10.1007/s10329-009-0153-2

28. Band R, Gnutzmann S. Quantum Graphs via Exercises. 2017

29. Garay-Ruiz D, Bo C. Chemical reaction network knowledge graphs: the OntoRXN ontology. *Journal of Cheminformatics* 2022; 14(1). doi: 10.1186/s13321-022-00610-x

30. Franceschet M. Collaboration in computer science: A network science approach. *Journal of the American Society for Information Science and Technology* 2011; 62(10): 1992–2012. doi: 10.1002/asi.21614

31. Kartal S, Gurcan F. Discretization of conformable fractional differential equations by a piecewise constant approximation. *International Journal of Computer Mathematics* 2018; 96(9): 1849–1860. doi: 10.1080/00207160.2018.1536782

32. Kartal S. Multiple bifurcations in an early brain tumor model with piecewise constant arguments. *International Journal of Biomathematics* 2018; 11(04): 1850055. doi: 10.1142/s1793524518500559

33. Kartal S. Flip and Neimark–Sacker bifurcation in a differential equation with piecewise constant arguments model. *Journal of Difference Equations and Applications* 2017; 23(4): 763–778. doi: 10.1080/10236198.2016.1277214

34. Kangalgil F. Neimark–Sacker bifurcation and stability analysis of a discrete-time prey–predator model with Allee effect in prey. *Advances in Difference Equations* 2019; 2019(1). doi: 10.1186/s13662-019-2039-y

35. Kangalgil F. Flip Bifurcation and Stability in a Discrete-Time Prey-Predator Model with Allee Effect. *Cumhuriyet Science Journal* 2019. doi: 10.17776/csj.509898

36. Zhao M, Xuan Z, Li C. Dynamics of a discrete-time predator-prey system. *Advances in Difference Equations* 2016; 2016(1). doi: 10.1186/s13662-016-0903-6

37. Mendes EMAM, Nepomuceno EG. A Very Simple Method to Calculate the (Positive) Largest Lyapunov Exponent Using Interval Extensions. *International Journal of Bifurcation and Chaos* 2016; 26(13): 1650226. doi: 10.1142/s0218127416502266

38. Nepomuceno EG, Martins SAM. A lower bound error for free-run simulation of the polynomial NARMAX. *Systems Science &amp Control Engineering* 2016; 4(1): 50–58. doi: 10.1080/21642583.2016.1163296

How to cite this article: Williams K., B. Hoskins, R. Lee, G. Masato, and T. Woollings (2016), A regime analysis of Atlantic winter jet variability applied to evaluate HadGEM3-GC2, *Q.J.R. Meteorol. Soc.*, *2017;00:1–6*.